Journal of Polymer Research (2020) 27: 247
https://doi.org/10.1007/s10965-020-02227-w

ORIGINAL PAPER

Effective removal of dyes from aqueous solutions using a novel antibacterial polymeric adsorbent

Faisal Suleiman Mustafa[1] · Mümtaz Güran[2] · Mustafa Gazi[1]

Received: 9 February 2020 / Accepted: 27 July 2020 / Published online: 4 August 2020

Abstract

Here, ethylenediamine-epichlorohydrin-trichlorophenol (EET) cross-linked polymer was synthesized and characterized by Fourier Transforms Infrared spectroscopy (FTIR), thermogravimetric analysis (TGA–DSC) and scanning electron microscopy (SEM). EET exhibited substantial antibacterial activity with inhibition zones of 38 and 64 mm against *E. coli* and *S. aureus* bacteria. Therefore, it was applied to treat methyl orange (MO) and rhodamine B (RB) dyes containing synthetic aqueous solutions under varying operation parameters. Notably, 10 and 15 mg of EET removed 98.72% of MO at pH 8 and 92.45% of RB at pH 3. Moreover, EET cross-linked polymer retained stable activities of about 98.6% over five consecutive recycling runs for MO dye. The EET demonstrated a fast adsorption rate and the adsorption data fits well with the pseudo-second-order for both dyes, suggesting chemisorption. Also, considering the correlation coefficient values, the experimental dataset fits suitably with Temkin equation for RB and Langmuir equation for MO. Thermodynamic evaluations for both dyes show spontaneity onto the cross-linked polymer.

Keywords Dye adsorption · Trichlorophenol · Polymer · Thermodynamic · Antimicrobial

Introduction

Water pollution emanating from textiles, paper and leather tanning industries is an increasing environmental problem [1]. Globally, ~10×10^3 dyes are available and used in different industries; the majority of these dyes remained in the water after the manufacturing processes and further released into the water sources [2–7]. Azo dyes like methyl orange (MO) is anionic and often used in textiles, food industries, pharmaceutical and printing shops [8]. Reports revealed that it is a carcinogenic, water-soluble, chemically stable and resistance to biodegradation [9, 10]. While rhodamine B (RB) a cationic dye is a fluorescent-based xanthine dye, usually used as tracking in pharmaceutical industries, paper printing and textile [11, 12]. Reports have shown that it is a carcinogenic, neurotoxic effects, also it causes respiratory and gastrointestinal tract irritation, and reproductive toxicity in both humans and animals [13]. Besides, several acute reactions to excessive oral exposure to RB have been reported with various types of skin rash [10]. The presence of a tiny amount of these dyes in water is apparent and unfavourable for the aquatic environment due to their toxicity and ability to inhibit light penetration [4–6]. Exposure to a concentrated dosage of the dyes is lethal and can trigger different diseases including cancer, lungs infection and dermatitis [7, 14].

Adsorption technique is widely used to remove dyes from solutions due to its simplicity, the non-selectivity and inexpensive nature [15]. The use of polymers as an adsorbent to extract dyes from wastewater has become favourable due to their eco-friendly nature, renewability and reported superior performance [16]. Note that not all polymers are eco-friendly; however, among bio-friendly polymers, chitosan has commonly been applied due to its non-toxic nature, biological and chemical properties.

✉ Faisal Suleiman Mustafa
faisal.mustafa@emu.edu.tr

✉ Mustafa Gazi
mustafa.gazi@emu.edu.tr

[1] Polymeric Materials Research Laboratory, Department of Chemistry, Faculty of Arts and Sciences, Eastern Mediterranean University, TR North Cyprus via Mersin 10, Famagusta, Turkey

[2] Department of Medical Microbiology, Faculty of Medicine, Eastern Mediterranean University, TR North Cyprus via Mersin 10, Famagusta, Turkey

Munagapati et al. [17] employed chitosan beads to extract 73 mg/g of MO from aqueous solution and suggested that the MO bound with the hydroxyl and protonated amino groups on the surface of chitosan [17]. Kaushal and Tiwari [18] adsorptively applied alginate beads to remove 0.08 mg/g of RB dye from the aqueous solution. Ethylenediamine-epichlorohydrin cross-linked polymer was prepared by condensation polymerization effectively adsorbed 11.7 mmol/g of nitrite ions [19], and also demonstrated high removal efficiency reactive brilliant red dye from wastewater which was ascribed to its hydrophilic and hydrophobic groups [20]. Poly(dimethylamine-co-ethylenediamine-co-epichlorohydrin) was used as a chelating agent for copper ions from wastewater [21]. It is worthy to mention that polymeric adsorbents have consistently demonstrated high performance in water treatment considering these numerous reports [17–22].

Note that the presence of pathogens in water is another serious problem limiting the accessibility to potable water resources. Even though the majority of the polymeric adsorbents have demonstrated sufficient adsorptive capability, very few possess antimicrobial activities. Like chitosan, chlorophenol compounds (like 2,4,5-trichlorophenol, TCP) have been applied as antiseptic agents due to their devastating antimicrobial activity [23]. However, they have limited application because of their potential toxicity [24].

To design a polymeric material with sufficient adsorption efficiency and substantial antimicrobial activity, ethylenediamine-epichlorohydrin-trichlorophenol (EET) cross-linked polymer was prepared in this study via a condensation polymerization technique. The physicochemical characters of the as-prepared EET were investigated and its adsorptive behaviour in the presence of methyl orange and rhodamine B dyes was established under varying conditions (pH, initial concentration, EET dosage and temperature). Furthermore, thermodynamics, Langmuir, Temkin and Freundlich adsorption isotherms, and adsorption kinetics of EET polymer were calculated. Besides, the inhibition growth of EET polymer was observed against *E. coli* and *S. aureus* bacteria. Also, the reusability tests of EET cross-linked polymer were studied over five repeated reuse cycles.

Materials and methods

Materials

Rhodamine B (RB, 479.02 g/mol), hydrochloric acid, 2,4,5-Trichlorophenol (TCP), epichlorohydrin (ECH), chloroform, ethylenediamine (EDA), sodium chloride and ethanol were brought from Sigma-Aldrich (USA). Methyl orange (MO, 327.33 g/mol) was purchased from (BDH) England. *Staphylococcus aureus* (*S. aureus*, ATCC 29213), *Escherichia coli* (*E. coli,* ATCC 25922). Triethylamine (TEA), acetone and Muller Hinton Agar (MHA) were purchased from Merck (Germany). MHA and bacteria were used in the disk diffusion antimicrobial test.

Synthesis of cross-linked polymer (EET)

In a 50 ml round bottom flask, 0.30 g of TCP was dissolved with 50 and 235 µl of EDA and ECH respectively, with the mole ratio of 2:1:4. Then, 1 ml of TEA was added as a base and the mixture was stirred at 250 rpm for 5 h at 85 °C. The product was formed; the base and the unreacted liquids were removed by a vacuum oven at 50 °C overnight. The product was washed by chloroform to remove unreacted components. EET cross-linked polymer (Fig. 1) was filtered and washed by water and acetone. Then, it was dried at 40 °C overnight (percentage yield 76.2%).

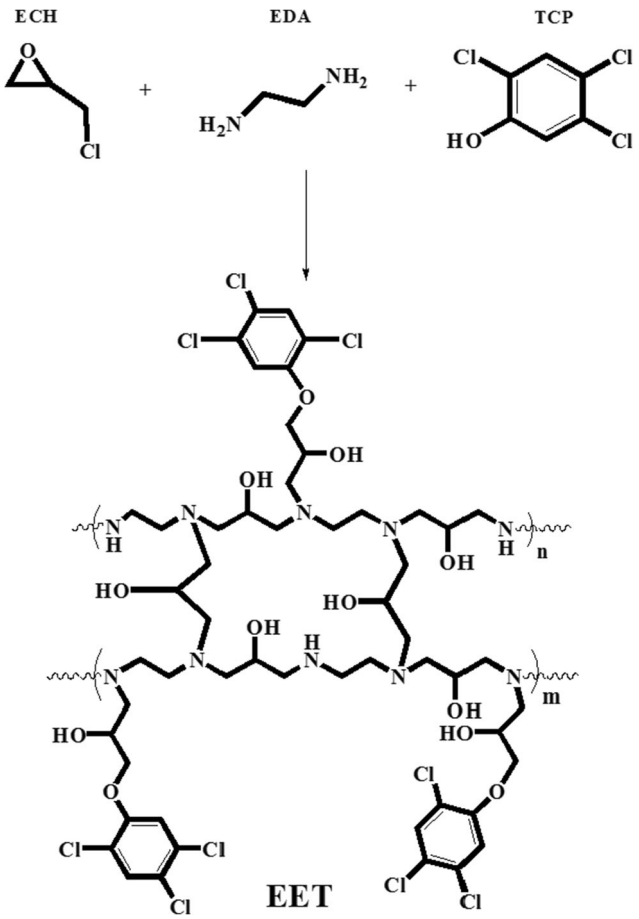

Fig. 1 Structure of EET cross-linked polymer

Adsorption experiments

All adsorption trials were performed at 200 rpm using 100 ml flask containing 25 ml of dye solutions. The effect of adsorption parameters such as pH (2–9), initial concentration (10–100 ppm), adsorbent dosage (10–20 g), reaction time (0–24 h) and effect of temperature (30–50 °C) were investigated. The pH of the solutions was adjusted by 0.1 M of HCl and 0.1 M NaOH. Results reported herein are the average of duplicate trials. After adsorption, the solution was filtered by filter paper, and the filtrate analyzed for residual MO and RB concentrations by UV-vis spectroscopy (T90+ Ultraviolet-visible spectrophotometer PG Instruments Ltd., UK) at the maximum wavelengths of 464 and 354 nm, respectively.

The concentrations were determined using a linear regression equation obtained by plotting a calibration curve of MO and RB absorption over a range of concentrations with $R^2 \geq 0.999$ for both MO and RB. The uptake capacity at any time or equilibrium (mg/g) and removal (%) of the polymer were calculated as described elsewhere [25]. To understand the adsorption mechanism, the pH point zero charge (pHzpc) of adsorbent was studied using a drift method as follows: initial pH (2–9) was adjusted by 0.1 mol/L NaOH or HCl. 10 mg of EET polymer was added individually for each pH and agitated at 298 K with contact time 24 h. In the end, the final pH of the solutions were measured and plotted vs initial pH [26], pH_{zpc} determined as 6.5 as shown in Fig. 2. The experimental results were fitted with three different isotherm linear models (Temkin, Freundlich and Langmuir) which have been described in detail [27]. Also, the thermodynamic behaviour at different temperatures was examined considering the following equations [28]:

$$K_c = \frac{q_e}{c_e} \tag{1}$$

$$\ln(K_c) = \left(\frac{\Delta S^o}{R}\right) + \left(\frac{\Delta H^o}{nRT}\right) \tag{2}$$

$$\Delta G^o = \Delta H^o - T\Delta S^o \tag{3}$$

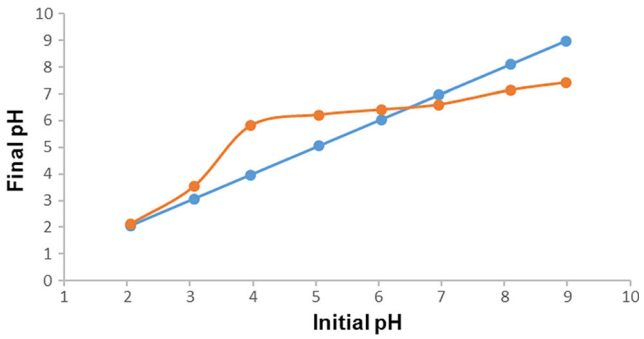

Fig. 2 Zero-point charge (pH_{zcp}) of EET polymer

Desorption and regeneration of cross-linked polymer

The desorption process of RB and MO dyes were performed using 10 mg of EET-loaded with MO and RB dyes individually in 25 ml of 0.1 M HCl and 25 ml of ethanol, respectively. The EET-loaded dyes were agitated at room temperature for 24 h at 200 rpm. Then the solutions were filtered and the residual MO and RB concentrations were analyzed by UV-vis spectroscopy at absorption wavelengths (286 and 354 nm) respectively. Afterwards, the adsorbent was washed by distilled water and dried at 40 °C, then subjected to successive reuse cycles under optimum conditions.

Disc diffusion assay

Disc diffusion assay was conducted by using standard strains of *E. coli* and *S. aureus* to test the antimicrobial activity of the cross-linked polymer. The inoculation of each bacteria strain with a concentration of 1×10^7 CFU/mL was done by using sterile swabs. After the bacteria were inoculated into the MHA, the polymer discs and empty discs were transferred on the agar plates for *E. coli* and *S. aureus* bacteria. Then, the agar plates were incubated at 37°C for 24 h under aerobic conditions. The zone of inhibition was measured in diameters.

Results and discussion

Characterization of EET cross-linked polymer

Thermogravimetric analysis and differential scanning calorimetry

The thermal properties of the EET were analyzed by TGA (HITACHI, STA7300, Japan) and DSC (204 F1: NETZSCH, Germany). Figure 3 shows the results of a) TGA and b) DSC of the polymer. Figure 3b shows an endothermic peak for the EET. Glass transition (T_g) appeared at −24.7 °C when the polymer changed from solid-state to a rubbery state. Peaks between 20 and 200 °C referred to change in the polymer states (from rubbery state to liquid state), this change is accompanied a change in density (when the density changes, the mass will change). The main peak of decomposition appeared between 273 to 400 °C. This result was supported by TGA (Fig. 3a). Around 1% weight loss of polymer occurred when the temperature increased to 195 °C. Beyond 200 °C, the weight loss gradually increased to 83% at 400 °C and stabilized at 86%. The decrease in mass% most probable was due to not only the degradation of the backbone (N-C, C-C) bonds in the polymer. Also, from the branches (trichlorophenol, C-C, C-O and C-H bonds), decomposition of chlorophenols moiety will form gases such as CO, CO_2,

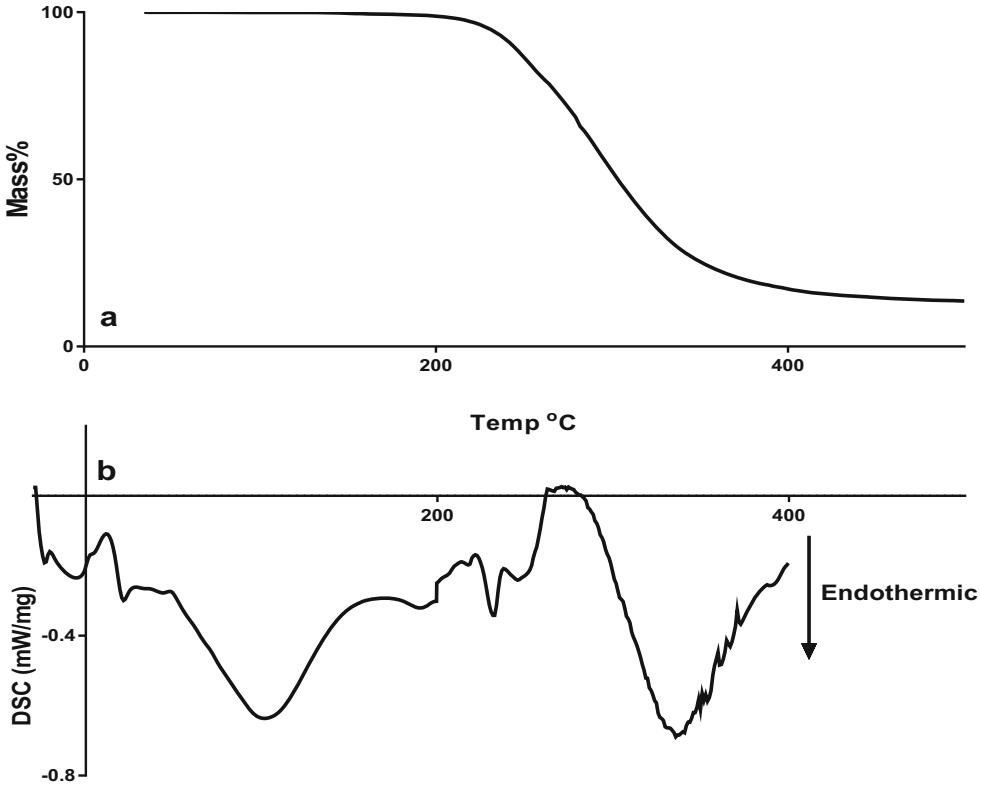

Fig. 3 **a**) TGA and **b**) DSC of the EET cross-linked polymer

Cl_2, and HCl [29]. It can be concluded from these results that the compound is thermally stable.

FT-IR results

Fourier Transform Infra-Red (FT-IR) (PerkinElmer, UK) was utilized to compare cross-linked polymer (EET) with EDA and ECH molecules as shown in Fig. 4. The amine groups were the main peaks of interest. It appeared at 1591 cm^{-1} in EDA spectra in Fig. 4a, however, its intensity decreased because it reacted with ECH in the main chain, cross-linked and branched with TCP. Some of the amines left as primary amine and appeared around 1600 cm^{-1} as shown in Fig. 4b. Peaks at 2926 and 2860 cm^{-1} referred to C − H in EDA in Fig. 4a, these peaks shifted and overlapped to 2948 and 2829 cm^{-1} in Fig. 4b. In the EET, new C − N peaks between EDA and ECH

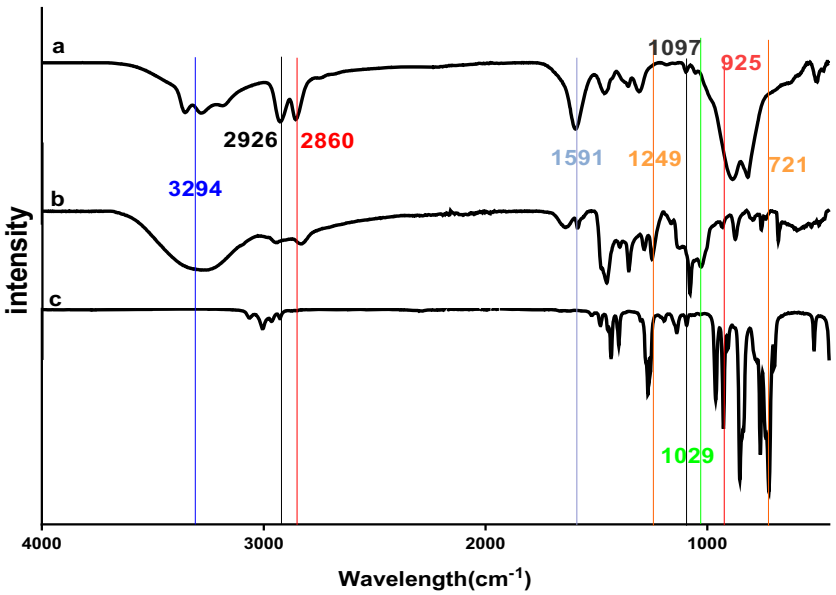

Fig. 4 FT-IR of a) EDA, b) EET cross-linked polymer and c) ECH

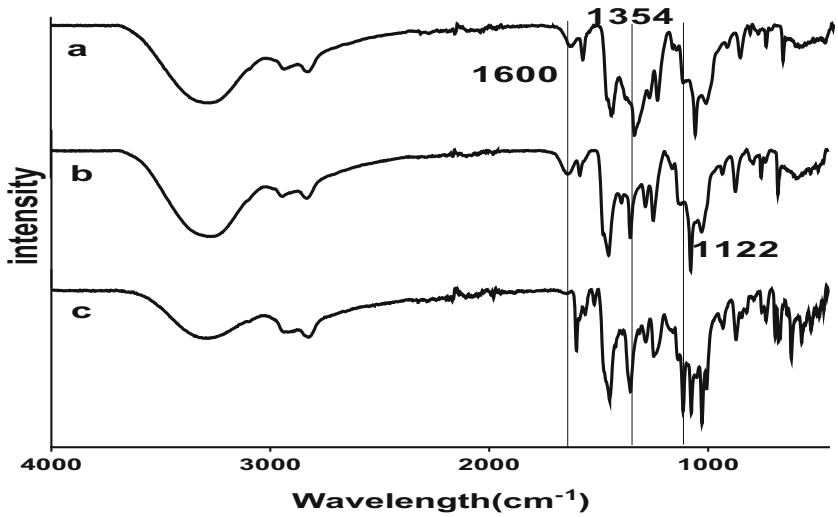

Fig. 5 FT-IR of a) polymer adsorbed RB dye, b) polymer before adsorption and c) polymer adsorbed MO dye

appeared at 1289 and 1249 cm^{-1}. The broad peak at 3294 cm^{-1} in Fig. 4b correlates with -OH and amine (-NH) [30]. The peak at 925 and 721 cm^{-1} correlate with (C-O-C) epoxy and (C-Cl) in ECH spectra Fig. 4c [31]. These peaks disappeared in the polymer (EET) see Fig. 4b, due to the reaction.

The last peak appeared at 1029 cm^{-1} in Fig. 4b referred to (C-O-C) ether in the branch between ECH and TCP [32]. Figure 5 shows the FT-IR spectrum of EET before (Fig. 5b) and after adsorption of MO (Fig. 5c) and RB (Fig. 5a) dyes. From Fig. 5c, the amine (N-H) bond around 1600 cm^{-1} disappeared, and the peak at 1122 cm^{-1} correlated to (S=O) in the MO molecule [33]. Peaks between 1000 and 1100 cm^{-1} changed because of the interaction between the EET and MO dye molecules. On the other hand, the peaks around 1350 cm^{-1} in Fig. 5a became wider due to the chemical interaction between nitrogen in the EET and oxygen in the carboxylate ion in RB dye molecules.

Determination of the polymer composition

The polymer formations were examined by elemental analysis (EuroEA3000, UK). The chlorine content of the EET was used to find the amount of TCP that reacted. Table 1 shows the percentage of each element; and found 4.99% of Nitrogen which indicated that all the amount of EDA had reacted with ECH in the polymer and 8.18% of chlorine (2.18×10^{-3} mol of TCP) reacted with ECH as a branch on the polymer.

Table 1 Elemental analysis of the EET cross-linked polymer

Sample	%C	%Cl	%N	%H
EET	35	8.18	4.99	44.33

SEM analysis

The surface morphologies of EET before and after adsorption of RB and MO were examined by SEM (FEITM.VERSA 3D, USA) and shown in Fig. 6a-c. The EET exhibited a rough surface and with visible pores of an average diameter of 2.86 μm (Fig. 6a) before adsorption. After the adsorption process of MO dye (Fig. 6b) and RB dye (Fig. 6c), the surface morphologies of EET showed that the majority of the pores were filled by the adsorbed dyes. Comparatively, the surface morphology of EET containing MO dye exhibited a less roughened topology than that of EET containing RB dye molecules. Noticeably, EET-RB exhibited a little rough surface with some unoccupied pores which might be attributed to the fact that RB is bulkier (479.02 g/mol) than MO dye (327.33 g/mol). The observation is consistent with the Freundlich isotherm results which suggested physisorption may contribute to RB adsorption.

Effect of initial solution pH

One of the critical parameter influencing pollutant adsorption is the solution pH; here, the performance of EET was investigated when the solution pH was varied from 2 to 9. Here, 10 mg EET was used in the presence of 10 ppm of MO and RB, at 298 K and contact time of 24 h. As shown in Fig. 7. The performance of EET is high at all pH but remarkable adsorption was achieved at pH 8; suggesting that both acidic and basic solutions are suitable for the removal of MO molecules. For MO dye, the removal percentage is 97% at pH 8 while the highest RB removal (70%) was attained at pH 3.

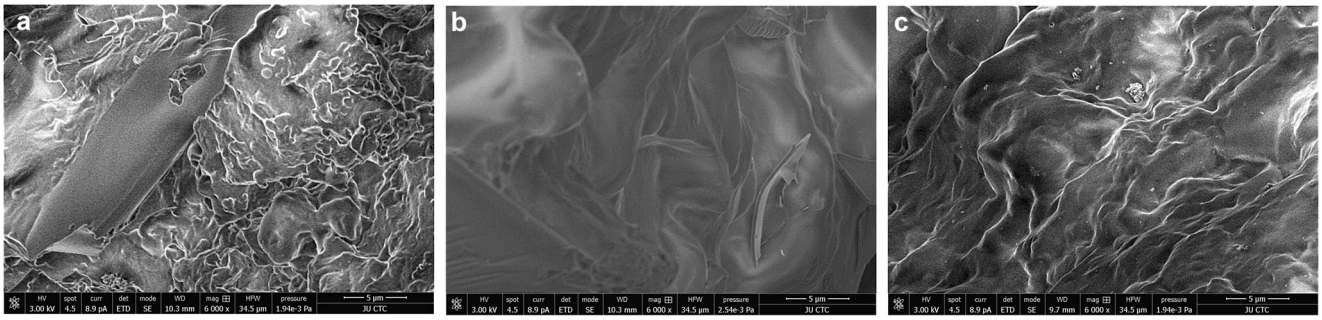

Fig. 6 SEM micrograph (×6000) of **a**) polymer before adsorption, **b**) polymer adsorbed MO dye and **c**) polymer adsorbed RB dye

The pH_{pzc} (the pH at which the surface charges on the adsorbent is zero) of EET was obtained as 6.5, which means at pH values lower than the pH_{pzc}, the surface of the EET will be positively charged and vice versa [34]. The adsorption of MO at the acidic medium is attributed to electrostatic interaction between the positively charged EET surface and the negatively charged sulphonic group of the MO. At alkaline condition. MO adsorption is not electrostatic but might be due to hydrophobic interaction or noncovalent π–π interactions between aromatic rings of the dye and that of the trichlorophenol, which is reflected in the FTIR spectra (Fig. 5). A similar observation has been reported elsewhere [35]. For RB, the adsorption at the acidic medium is likely due to hydrophobic, π–π interactions or interaction between the protonated amino group on the polymer and the carboxylate ions on RB. EET exhibited a wide performance until beyond pH 8, where the RB removal decreased remarkably which is attributed to the electrostatic repulsion between the negative charged EET and the zwitterionic form of RB in solution [18, 36, 37].

Effect of adsorbent dosage

The effect of adsorbent dosage is illustrated in Fig. 8. Only slight increases in the removal of MO was noticed when the EET dosage increased. Particularly, the removal increased from 92.5% to 94.0% when the dosage was increased from 10 to 20 mg. On the other hand, noticeable increases in the removal of RB was seen when the EET dosage increased; the RB removal increased from 65% to 80% when the amount was increased from 10 to 20 mg.

Effect of initial concentration

The effect of initial dye concentration on the removal efficiency of MO and RB dye solutions in the concentration range of 10–100 ppm is shown in Fig. 9. As MO dye solution concentration increased from 10 to 100 ppm, the uptake capacity increased from 22.74 to 240.71 mg/g, while RB dye uptake increased from 11.24 to 126.30 mg/g. The increasing trend of uptake capacity is attributed to the driving force of the concentration with increasing initial dye concentration [18]. A similar observation was noticed by Oladipo and Ifebajo [34], they reported that a high concentration of rhodamine B dye facilitated a higher mass transfer driving flux. Hence more RB species were transported from the aqueous solution to the adsorbent surface, which resulted in a higher RB removal.

Adsorption isotherm

The experimental results were fitted with Langmuir, Temkin and Freundlich models; obtained parameters are presented in

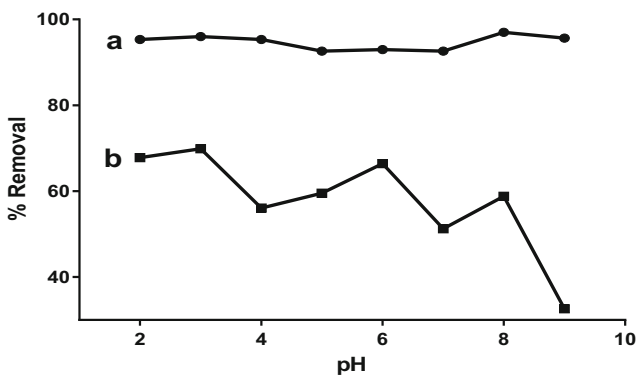

Fig. 7 Effect of pH on a) MO and b) RB adsorptions

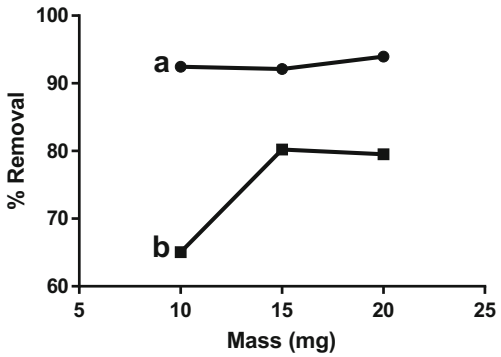

Fig. 8 Effect of dosage vs % Removal of a) MO (20 ppm, pH 8.0 ± 0.1) and b) RB (10 ppm, pH 3.0 ± 0.1) at room temperature

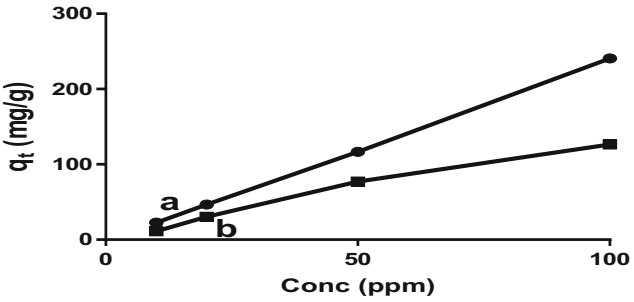

Fig. 9 Effect of concentration of dye solutions, a) MO (pH 8.0 ± 0.1) and b) RB (pH 3.0 ± 0.1) vs intake capacity. Amount of polymer 10.0 mg, volume of solutions 25 ml and temperature room temperature

Table 2. Considering the correlation coefficient value, the Langmuir isotherm model is suitable to describe the adsorption process of MO with $R^2 > 0.998$. This implies that the EET contained active functional groups that are uniformly distributed and with the same energy level and thus initiate a monolayer coverage of the dye molecules via chemisorption mechanism [38]. However, RB adsorption is best described by Temkin $R^2 = 0.9990$ compared to the Langmuir which R^2 is 0.9777 and Freundlich models with $R^2 = 0.9911$. According to Temkin model, the adsorption energy diminishes directly with the surface covering of EET polymer because of adsorbate-adsorbent interaction (chemisorption system) [27, 34, 39, 40].

Effect of temperature and thermodynamic parameters

The performance of EET was examined at three different temperatures (303, 313 and 323 K) and the thermodynamic parameters including enthalpy change (ΔH^o), free Gibbs energy change (ΔG^o) and entropy change (ΔS^o) were calculated. The removal efficiencies of MO and RB decreased with increasing temperature which is consistent with the data listed in Table 3, where the adsorption of MO and RB is noted to be exothermic due to negative values of ΔH^o. The negative value of ΔS^o for RB adsorption indicates a decrease in the degree of randomness of the RB dye molecule at the solid-liquid interface during the adsorption process. The positive ΔS^o value of MO denotes an increase in the degree of randomness since heat is not transferred from the environment to the system (ΔH^o is negative) which is isolated, therefore the entropy is considered as the main driving force for adsorption This value was expected since MO molecule is anionic (has a negative charge) and the dye solution is basic (pH = 8) with a negative charge, leading to a significant repulsion between the negative charges of the solution and the dye molecules which results in rising of ΔS^o value (positive). Moreover, the values of ΔG^o at all temperatures for both dyes are negative which revealed the spontaneity of the adsorption process [28, 41].

Table 3 Thermodynamic parameters of the adsorption of MO and RB Dyes onto EET cross-linked polymer

	ΔG^o (KJ/mol)			ΔH^o (KJ/mol)	ΔS^o (J/mol.K)
	303 K	313 K	323 K		
Methyl Orange (MO)	−9.849	−9.884	−9.918	−8.814	+3.417
% Removal	95.26	94.62	94.18		
Rhodamine B (RB)	−7.870	−6.223	−4.576	−57.768	−164.68
% Removal	93.56	85.21	77.90		

Kinetics studies

Figure 10 shows the adsorption rate of MO and RB dyes when 10 and 15 mg of EET were used to remove 50 ppm of the MO and RB dye solutions respectively. The removal of the dyes was rapid where more than 50% was removed after 15 mins for MO and 50 mins for RB dye. Note that MO removal rate reached equilibrium after 4 h to with more than 98% removal, while 91% of RB was removed after 12 h. The experimental results were fitted into the pseudo-first-order and pseudo-second-order kinetic models and obtained parameters are given in Table 4. Considering the correlation coefficient and calculated q_e, the pseudo-second-order model fits well with the experimental results. Specifically, the correlation coefficient of the pseudo-second-order model (R^2 of MO and RB ≥

Table 2 Adsorption isotherms parameters of MO and RB onto EET cross-linked polymer

Dye type	Langmuir $\frac{c_i}{q_e} = \frac{c_e}{q_{max}} + \frac{1}{k_L . q_{max}}$			Freundlich $Log(q_e) = Log(K_F) + \left(\frac{1}{n}\right)\log(c_e)$			Temkin $q_e = \left(\frac{RT}{b_T}\right)(\ln(c_e) + \ln(k_T))$		
	q_{max}	b_L	R^2	K_F	n	R^2	b_T	K_T	R^2
MO	144.9	0.56	0.9986	29.57	0.7	0.8687	110.1	4.1	0.9866
RB	149.3	0.24	0.9770	41.57	2.1	0.9911	43.7	1.0	0.9990

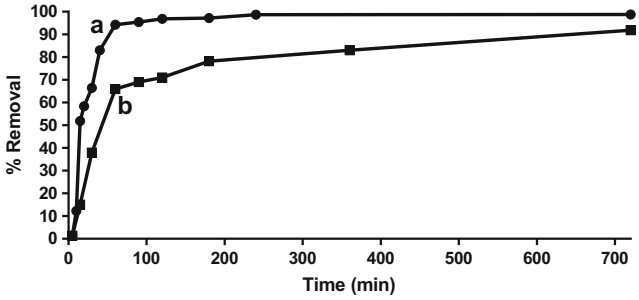

Fig. 10 Effect of contact time on percent removal of a) MO dye solution (50 ppm, pH 8.0, 10.0 mg) and b) RB dye solution (50 ppm, pH 3.0, 15.0 mg) at room temperature

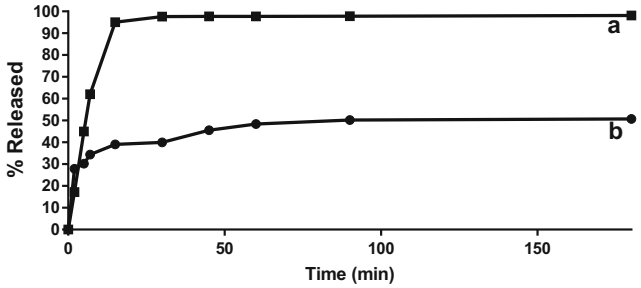

Fig. 11 Releasing of a) MO from polymer by (0.1 M HCl) and b) RB from polymer by ethanol

0.99) is higher than that of the pseudo-first-order model (R^2 of MO ≥ 0.97 and RB ≥ 0.98). Also, the theoretical q_e values of pseudo-second order are nearer to the experimental values, suggesting chemisorption.

Desorption and regeneration of cross-linked polymer

The desorption of the adsorbed dyes from the polymer was investigated by using 0.1 M HCl and ethanol as eluents for MO and RB dyes, respectively. Clearly from Fig. 11a, more than 50% of MO was desorbed after 5 mins from the EET which extended to 98% after 45 mins. Contrastingly, only 51% of RB dye was desorbed after 90 mins as presented in Fig. 11b. The reuse of the desorbed EET was evaluated after thermal treatment at 40 °C Table 5. EET maintained sufficiently high performance even after 5 recycle uses (98.72–98.65%) within 4 h. In comparison, the removal efficiency for RB decreased from 92.45% to 47.39% after consecutive reuse within 24 h. It is worthy to note that EET efficiency decreased by 45.1% after reused twice for RB adsorption, suggesting it has higher affinity and remarkable adsorptive potential for MO, which may be due to its lower molecular weight (327.3 g/mol) compared to the larger (479.02 g/mol) RB dye. The performance of EET is compared with other reported polymeric adsorbents in the literature as presented in Table 6. As noted, EET performance is superior; for instance, Bahrudin et al. [42] reportedly applied polyaniline to remove MO dye and achieved 125 mg/g at pH 6.5, likewise, Allouche et al. [43] reported that chitosan only achieved 29 mg/g removal of MO from the aqueous solution at pH 3.0. EET efficiency is higher than the modified Moroccan clay containing cetyltrimethylammonium bromide, which removed 78.74 mg/g of RB dye at pH 7.

Table 4 Kinetic parameters of Methyl Orange and Rhodamine B Adsorption onto EET polymer

Type of dye	1st Order $\ln(q_e - q_t) = \ln(q_e) - k_1 \cdot t$				2nd Order $\left(\frac{t}{q_t}\right) = \left(\frac{1}{k_2 \cdot q_e^2}\right) - \left(\frac{t}{q_e}\right)$				q_e (Exp)(mg/g)
	q_e (mg/g)	k_1 (min^{-1})	R^2	$q_e - q_t$(mg/g)	q_e (mg/g)	k_2 (g/mg.min)	R^2	$q_e - q_t$ (mg/g)	
RB	43.88	0.0064	0.97	−33.17	80	0.000311	0.9985	2.95	77.05
MO	129.31	0.0396	0.982	5.9	133.33	0.000553	0.9957	9.92	123.41

Table 5 % Removal of MO and RB dye solutions by reuse the cross-linked polymer

Number of repetition	% Removal of MO dye solution	% Removal of RB dye solution
1st	98.72	92.45
2nd	98.66	47.39
3rd	98.66	–
4th	98.65	–
5th	98.65	–

Table 6 Comparison of the adsorption capacities of various adsorbents towards Methyl Orange and Rhodamine B Dyes

	Adsorbent	Experimental conditions	q_{max} (mg/g)	Refs
MO	Activated carbons of corncob derived char wastes	pH 7, 298 K	11.57	[44]
	Graphene oxide	pH 3, 298 K	16.83	[45]
	Chitosan	pH 3, 298 K	29	[46]
	Chitosan intercalated montmorillonite	pH 2, 328.2 K	123.46	[47]
	Polyaniline	pH 6.5, 303	125	[48]
	EET cross-linked polymer	pH 8, 298 K	144.9	This work
RB	Paper industry waste sludge	pH 2.4, 308 K	6.711	[49]
	poly (ethylene terephthalate) fibers grafted by 4-vinyl pyridine and 2-methylpropenoic acid	pH 12, 298 K	45.28	[50]
	Poly(cyclotriphosphazene-co-4,4′-sulfonyldiphenol) Nanotubes	pH 1.2298 K	46.06	[51]
	Modified Moroccan Clay with Cetyltrimethylammonium Bromide	pH 7, 298 K	78.74	[52]
	zinc oxide loaded activated carbon (ZnO-AC)	pH 7, 303 K	128.21	[53]
	EET cross-linked polymer	pH 3, 298 K	149.3	This work

Disc diffusion assay

Disc diffusion method was used to determine antimicrobial activity with *E. coli* and *S. aureus* bacteria by measuring the zones of the inhibition of EET cross-linked polymer. Figure 12 shows the result of this inhibition with 39 and 64 mm inhibition zone with *E. coli* and *S. aureus* bacteria. The antibacterial activities of EET are attributed to the presence of chlorine atoms (from trichlorophenol), hydroxyl and amine groups (in the backbone of the polymer). The protonated amino groups can interact electrostatically with the gram-negative bacteria strain and inhibit its growth. The chlorine can interact with the bacterial lipids within the cell walls and destroys the enzymes, hence, making the bacteria cells to be oxidized, and results to death. From these results, EET is a potential antimicrobial polymer with sufficient adsorption performance.

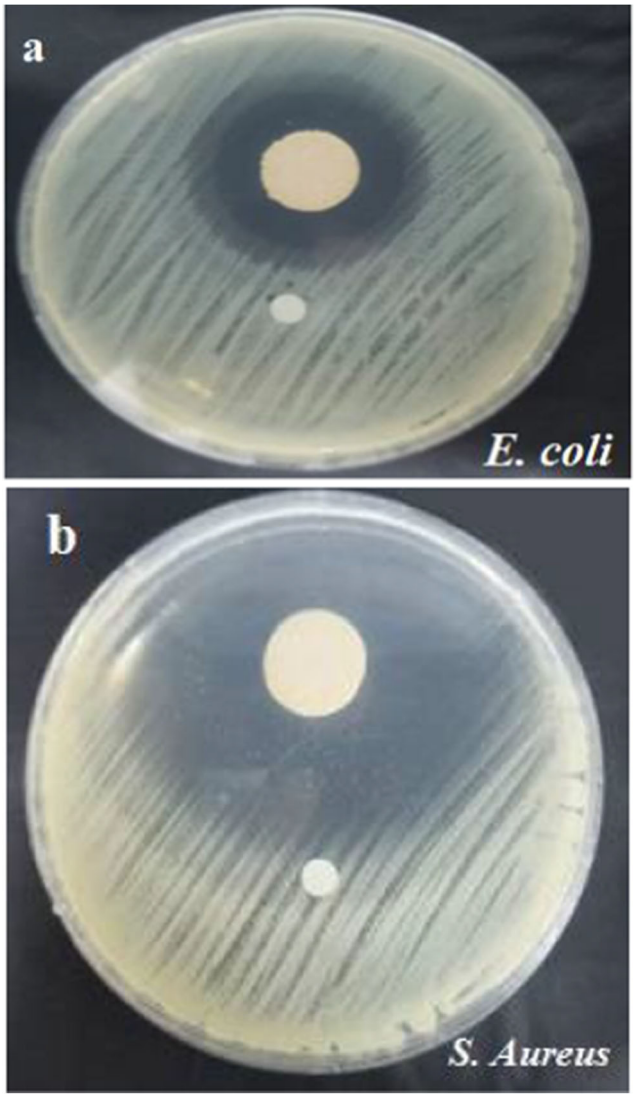

Fig. 12 Disk diffusion assay for **a**) *E. coli* and **b**) *S. aureus* bacteria

Conclusion

Herein, an ethylenediamine-epichlorohydrin-trichlorophenol cross-linked polymer (EET) was synthesized and characterized. The performance of EET for the treatment of dye-containing synthetic solutions was investigated for the removal of both anionic dye (methyl orange) and cationic dye (rhodamine B). 98.72% and 92.45% of MO and RB dyes were adsorbed at pH 8 and 3 using 10 mg and 15 mg of EET, respectively. Notably, more than 50% of MO was adsorbed during the first 15 min, which revealed that EET exhibited fast adsorption kinetically. According to the Langmuir isotherm, the maximum uptake of MO and RB is 145 mg/g and 149.3 mg/g under the optimum conditions. 98% of MO was desorbed by 0.1 M HCl from the spent EET after 45 min, while only 51% of

RB was desorbed within 90 min by ethanol. The regenerated EET maintained high removal efficiency (~98.65%) after 5 recycling circles. Also, the toxicity of the prepared polymer was eliminated due to its insoluble property, and EET exhibited excellent antimicrobial activities against *E. coli* and *S. aureus* with inhibition zones of 39 and 64 mm respectively via the disk diffusion assay. Results herein show that EET is an alternative polymeric adsorbent with antimicrobial functions for the treatment of dye contaminated industrial effluents.

Acknowledgements We thank Dr. Fadwa Odeh (The University of Jordan, Chemistry Department) and Dr. Walhan Alshaer (The University of Jordan, Cell Therapy Center) for helping us to characterize our polymer. The authors acknowledge the suggestions, editing and professional support received during manuscript curation and revision from Associate Professor Akeem Oladipo (Chemistry Department of Eastern Mediterranean University).

References

1. Ratnamala GM, Shetty KV, Srinikethan G (2012) Removal of remazol brilliant blue dye from dye-contaminated water by adsorption using red mud: equilibrium, kinetic, and thermodynamic studies. Water Air Soil Pollut 223(9):6187–6199
2. Gong R, Li M, Yang C, Sun Y, Chen J (2005) Removal of cationic dyes from aqueous solution by adsorption on peanut hull. J Hazard Mater 121(1–3):247–250
3. Chequer FMD, de Oliveira GAR, Ferraz ERA, Cardoso JC, Zanoni MVB, de Oliveira DP (2013) Textile dyes: dyeing process and environmental impact. Eco-friendly Text Dye Finish 6:151–176
4. Jain R, Sikarwar S (2006) Photocatalytic and adsorption studies on the removal of dye Congo red from wastewater. Int J Environ Pollut 27(1–3):158–178
5. Koprivanac N, Kušić H (2009) Hazardous organic pollutants in colored wastewaters. Nova Science Publishers
6. Mishra G, Tripathy M (1993) A critical review of the treatment for decolorization of dye wastewater. Colourage 40:35–38
7. Tahir H, Sultan M, Akhtar N, Hameed U, Abid T (2016) Application of natural and modified sugar cane bagasse for the removal of dye from aqueous solution. J Saudi Chem Soc 20: S115–S121
8. Hassanzadeh-Tabrizi SA, Motlagh MM, Salahshour S (2016) Synthesis of ZnO/CuO nanocomposite immobilized on γ-Al_2O_3 and application for removal of methyl orange. Appl Surf Sci 384: 237–243
9. Moazami A, Montazer M, Dolatabadi MK (2018) Rapid discoloration of methyl orange in water by conductive cu/Cu_2O/rGO modified polyester fabric. J Polym Environ 26(6):2502–2513
10. Xin Q, Fu J, Chen Z, Liu S, Yan Y, Zhang J, Xu Q (2015) Polypyrrole nanofibers as a high-efficient adsorbent for the removal of methyl orange from aqueous solution. J Environ Chem Eng 3(3): 1637–1647
11. Oladipo AA, Ifebajo AO, Nisar N, Ajayi OA (2017) High-performance magnetic chicken bone-based biochar for efficient removal of rhodamine-B dye and tetracycline: competitive sorption analysis. Water Sci Technol 76(2):373–385
12. Geng T-M, Wu D-Y, Huang W, Huang R-Y, Wu G-H (2014) Fluorogenic detection of Hg^{2+}, Cd^{2+}, Fe^{2+}, Pb^{2+} cations in aqueous media by means of an acrylamide-acrylic acid copolymer chemosensor with pendant rhodamine-based dyes. J Polym Res 21(3):354–362
13. Imam SS, Babamale HF (2020) A short review on the removal of rhodamine b dye using agricultural waste-based adsorbents. AJOCS 7(1):25–37
14. Kadirvelu K, Karthika C, Vennilamani N, Pattabhi S (2005) Activated carbon from industrial solid waste as an adsorbent for the removal of rhodamine-B from aqueous solution: kinetic and equilibrium studies. Chemosphere 60(8):1009–1017
15. Crini G, Lichtfouse E, Wilson LD, Morin-Crini N (2018) Adsorption-oriented processes using conventional and non-conventional adsorbents for wastewater treatment. In: Green Adsorbents for Pollutant Removal. Springer 23–71
16. Saberi A, Alipour E, Sadeghi M (2019) Superabsorbent magnetic Fe_3O_4-based starch-poly (acrylic acid) nanocomposite hydrogel for efficient removal of dyes and heavy metal ions from water. J Polym Res 26(12):271–285
17. Munagapati VS, Yarramuthi V, Kim DS (2017) Methyl orange removal from aqueous solution using goethite, chitosan beads and goethite impregnated with chitosan beads. J Mol Liq 240:329–339
18. Kaushal M, Tiwari A (2010) Removal of rhodamine-B from aqueous solution by adsorption onto crosslinked alginate beads. J Dispers Sci Technol 31(4):438–441
19. Biçaak N, Şenkal BF (1998) Removal of nitrite ions from aqueous solutions by cross-linked polymer of ethylenediamine with epichlorohydrin. React Funct Polym 36(1):71–77
20. Sun C, Zhang X, Zhang Z, Zhang Y (2013) Color removal from dyeing wastewater by the polymer of epichlorohydrin-ethylenediamine. Adv Mater Res 752:1448–1451
21. Molinari R, Argurio P, Poerio T (2004) Comparison of polyethylenimine, polyacrylic acid and poly(dimethylamine-co-epichlorohydrin-co-ethylenediamine) in Cu^{2+} removal from wastewaters by polymer-assisted ultrafiltration. Desalination 162(1–3): 217–228
22. Chunhui D, Xinyi Z, Xumin M (2020) The surface tunability and dye separation property of PVDF porous membranes modified by P(MMA-b-MEBIm-Br): effect of poly (ionic liquid) brush lengths. J Polym Res 29(79):1–11
23. Nendza M, Seydel JK (1990) Application of bacterial growth kinetics to in vitro toxicity assessment of substituted phenols and anilines. Ecotoxicol Environ Saf 19(2):228–241
24. Michałowicz J, Duda W (2007) Phenols - sources and toxicity. Pol J Environ Stud 16(3):347–362
25. Oladipo AA, Gazi M (2015) Two-stage batch sorber design and optimization of biosorption conditions by Taguchi methodology for the removal of acid red 25 onto magnetic biomass. Korean J Chem Eng 32(9):1864–1878
26. Alkan M, Doğan M (2001) Adsorption of copper (II) onto perlite. J Colloid Interface Sci 243(2):280–291
27. Nakhjiri MT, Marandi GB, Kurdtabar M (2018) Effect of bis [2-(methacryloyloxy) ethyl] phosphate as a crosslinker on poly (AAm-co-AMPS)/Na-MMT hydrogel nanocomposite as potential adsorbent for dyes: kinetic, isotherm and thermodynamic study. J Polym Res 25:244–263
28. Alokour M, Yilmaz E (2019) Photoinitiated synthesis of poly (poly (ethylene glycol) methacrylate-co-diethyl amino ethyl methacrylate) superabsorbent hydrogels for dye adsorption. J Appl Polym Sci 136(26):47707–47724
29. Kennedy MV, Stojanovic BJ, Shuman JFL (1972) Chemical and thermal aspects of pesticide disposal. J Environ Qual 1:63–65
30. Segal L, Eggerton FV (1961) Infrared spectra of ethylenediamine and the dimethylethylenediamines. Appl Spectrosc 15(4):116–117
31. Jiao M, Yang K, Cao J, Diao Q, Zhang W, Yu M (2016) Influence of epichlorohydrin content on structure and properties of high-ortho phenolic epoxy fibers. J Appl Polym Sci 133(18):43375–43381

32. González MG, Cabanelas JC, Baselga J (2012) Applications of FTIR on epoxy resins-identification, monitoring the curing process, phase separation and water uptake. Infrared Spectrosc Sci Eng Technol 2:261–284
33. Zhan C, Chen F, Dai H, Yang J, Zhong M (2013) Photocatalytic activity of sulfated Mo-doped TiO2@fumed SiO_2 composite: a mesoporous structure for methyl orange degradation. Chem Eng J 225:695–703
34. Oladipo AA, Ifebajo AO (2018) Highly efficient magnetic chicken bone biochar for removal of tetracycline and fluorescent dye from wastewater: two-stage adsorber analysis. J Environ Manag 209:9–16
35. Umpuch C, Sakaew S (2013) Removal of methyl orange from aqueous solutions by adsorption using chitosan intercalated montmorillonite. J Sci Technol 35(4):451–459
36. Li Q, Tang X, Sun Y, Wang Y, Long Y, Jiang J, Xu H (2015) Removal of rhodamine B from wastewater by modified volvariella volvacea: batch and column study. RSC Adv 5(32):25337–25347
37. Venkatraman BR, Gayathri U, Elavarasi S, Arivoli S (2012) Removal of rhodamine B dye from aqueous solution using the acid activated cynodon dactylon carbon. Der Chem Sin 3(1):99–113
38. Bazrafshan E, Zarei AA, Nadi H, Zazouli MA (2014) Adsorptive removal of methyl orange and reactive red 198 dyes by moringa peregrina ash. Indian J Chem Technol 21(2):105–113
39. Türkcan C, Uygun DA, Akgöl S, Denizli A (2014) Reactive red 120 and NI (II) derived poly (2-hydroxyethyl methacrylate) nanoparticles for urease adsorption. J Appl Polym Sci 131(2):39757–39764
40. Al-Ghouti MA, Da'ana DA (2020) Guidelines for the use and interpretation of adsorption isotherm models: a review. J Hazard Mater 393:1223834–1223856
41. Paiwei L, Xin D, Qilin Y, Zhenxi W, Shangxi Z, Meng C (2020) A novel modification method for polystyrene microspheres with dithizone and the adsorption properties for Pb^{2+}. J Polym Res 27(195):1–10
42. Bahrudin NN, Nawi MA, Ismail WINW (2018) Physical and adsorptive characterizations of immobilized polyaniline for the removal of methyl orange dye. Korean J Chem Eng 35(7):1450–1461
43. Allouche F-N, Yassaa N, Lounici H (2015) Sorption of methyl orange from aqueous solution on chitosan biomass. Procedia Earth Planet Sci 15:596–601
44. Hou X-X, Deng Q-F, Ren T-Z, Yuan Z-Y (2013) Adsorption of Cu2+ and methyl orange from aqueous solutions by activated carbons of corncob-derived char wastes. Environ Sci Pollut Res 20(12):8521–8534
45. Robati D, Mirza B, Rajabi M et al (2016) Removal of hazardous dyes-BR 12 and methyl orange using graphene oxide as an adsorbent from aqueous phase. Chem Eng J 284:687–697
46. Allouche F-N, Yassaa N, Lounici H (2015) Sorption of methyl orange from aqueous solution on chitosan biomass. Procedia Earth Planet Sci 15:596–601
47. Umpuch C, Sakaew S (2013) Removal of methyl orange from aqueous solutions by adsorption using chitosan intercalated montmorillonite. Songklanakarin J Sci Technol 35(4):451–459
48. Bahrudin NN, Nawi MA, Ismail WINW (2018) Physical and adsorptive characterizations of immobilized polyaniline for the removal of methyl orange dye. Korean J Chem Eng 35(7):1450–1461
49. Thakur A, Kaur H (2017) Response surface optimization of Rhodamine B dye removal using paper industry waste as adsorbent. Int J Ind Chem 8(2):175–186
50. Arslan M, Günay K (2018) Synthesis and use of PET fibers grafted with 4-vinyl pyridine and 2-methylpropenoic acid for removal of rhodamine B and methylene blue from aqueous solutions. J Polym Sci Appl 2(1):2
51. Wang M, Fu J, Zhang Y et al (2015) Removal of rhodamine B, a cationic dye from aqueous solution using poly (cyclotriphosphazene-co-4, 4′-sulfonyldiphenol) nanotubes. J Macromol Sci Part A 52(2):105–113
52. Damiyine B, Guenbour A, Boussen R (2017) Rhodamine B adsorption on natural and modified moroccan clay with cetyltrimethylammonium bromide: Kinetics, equilibrium and thermodynamics. J Mater Environ Sci 8(3):860–871
53. Saini J, Garg VK, Gupta RK, Kataria N (2017) Removal of Orange G and Rhodamine B dyes from aqueous system using hydrothermally synthesized zinc oxide loaded activated carbon (ZnO-AC). J Environ Chem Eng 5(1):884–892